International Research Journal of Engineering and Technology (IRJET) e-ISSN: 2395-0056
Volume: 08 Issue: 04 | Apr 2021 www.irjet.net p-ISSN: 2395-0072

CFD Investigation on the Circular Rectangular and Ellipse shape on the Aerodynamics in S-Duct

Amal RK[1], Akil Ahmed A[2], Abinesh N[3], Eben devaraj S[4]

[1-3]*Student, Department of Mechanical Engineering, Ponjesly College of Engineering, Nagercoil-629003*
[4]*Assistant professor, Department of Mechanical Engineering, Ponjesly College of Engineering, Nagercoil-629003*

Abstract - *The purpose of this paper is to design an S-duct intake for Aircraft and Automobile applications with good efficiency in a wide range of operating conditions. A fully-parametric 3-D CAD model (Catia) of the intake was constructed in order to produce different intake configurations, within specific geometric constraints, and to study the influence of geometry cross sectional variation on efficiency. Cylindrical-type, Rectangle- type and Ellipse- type blocking methodology was adopted in order to construct the block-structured mesh of hexahedral elements, used in the simulations. The commercial CFD code ANSYS-CFX was used to compute the flow field inside the flow domain of each case considered. The CFD analysis finds are Pressure, velocity, Kinetic energy, Density, Drag and lift forces. By shortening the axial length the flow separation after the first turning becomes more pronounced and the losses are increasing. For very long ducts the increased internal wall area leads to increased wall friction and, consequently, to increased loss production. The adoption of Gerlach-shaped profiles for the design of the S-duct resulted in a low pressure loss level for the optimal shape, although more uniform distribution of total pressure losses resulted for ducts longer than the optimal one, which should be taken into account in the design process.*

INTRODUCTION

A curved diffuser called an S-duct or S-bend is used to route air from the side of the flight vehicle to the other side.The nose of the F1 car to enhance its aerodynamic performance.In 2013 Sauber F1 team(C23) & Redbull F1 team(RB9) used this radical design on their respective cars. The cross sectional shape of an inlet can transition from rectangular, Circular, oval, etc. The duct centre line curvature can have different turning angles and shapes. The design varies depending upon the complete flight vehicle configuration.

THE PROBLEM

Whenever air flows over a surface, it loses energy, which causes the flow to slow down and become turbulent or 'dirty'. One of the main areas where this occurs is around the front wing. As air flows through the gap between the underside of the nose, the upper surface of the front wing and the inner faces of the front wing pillars an expanding tube of turbulent air is created. To make matters worse, the air that impacts the top corners of the nose then accelerates round and rolls underneath; adding to this turbulent tube of air that then continues downstream. The air flowing through the area is turbulent and to mitigate it's effect, the F1 S-duct was developed

F1 S-DUCT INLET

The inlets for the F1 S-duct are usually NACA ducts. This is a type of inlet which allows the air to be drawn in with high efficiency and minimal drag.

To achieve this, NACA ducts are usually placed parallel to the local airflow and in locations where the boundary layer is relatively thin.

The geometry of the NACA duct is essential in inducing air efficiently.

The shape and design of these NACA ducts encourages vortices to form, reducing static pressure and enhancing the efficiency of the flow through the inlet.

As air flows towards the narrow end of the duct, it flows down the gentle slope and into the inlet.

F1 S-DUCT OUTLET

Once the air has entered the S- ducts on the side of the nose, it is channelled through to the F1 S-duct outlet which is situated at the bridge of the nose.

This outlet can often be misinterpreted as a device to help avoid flow separation.

However, this outlet simply allows for the turbulent airflow surrounding the nose to be extracted and directed towards the cockpit where it will do the least damage to the overall car's aerodynamic performance.

APPLICATION

External aerodynamics:

- **Aircrafts** (involving subsonic, trans-sonic and supersonic wing design, spoilers, tailplane, Nose cone, landing gear etc),
- **Launch vehicles/missiles** (nose, fins etc)
- **Spacecraft design** (planetary missions to heavenly bodies with atmosphere, example Mars missions involving entry descend and landing) or capsules involving Earth re-entry missions (example Space shuttle, Orion, asteroid sample return missions)

Benefits and drawbacks

- The S-duct was invented as a solution for positioning the central engine on trijets. The S-duct was easier to service than alternative trijet designs. Most trijet designs opted for the S-duct layout. Only the McDonnell Douglas DC-10 and MD-11 trijets' designers chose not to use the S-duct and go with a "straight-through" layout.
- The straight-through layout leaves the engine high above the ground, making access difficult. The straight layout also increases total aircraft aerodynamic drag by 2–4%.
- Compared to an "in tail" design like on the DC-10 and MD-11, the S-duct allows a shorter fin and a rudder closer to the longitudinal axis.
- On the Lockheed L-1011 TriStar, engineers were able to maintain engine performance comparable with straight-through designs by limiting the curve of the S-duct to less than a quarter of the radius of the engine intake diameter.
- The S-duct design also reduced the total empty aircraft weight. The research undertaken during the design of the L-1011 indicated that losses of using an S-duct were more than compensated for by the above savings.

Experimental works

In order to investigate the importance of the various geometric parameters on the flow quality inside and outside an S-duct, a fully-parametric 3D CAD model of the intake was constructed, using CATIA V5 CAD software. In this parametric model the duct is constructed around a reference curve, which will be called centre line. This curve consists of three parts; the central one is a quadratic B-Spline curve, defined by four control points. Its control polygon is shown , using a dashed line. A straight line extension is added at the end of the B-Spline curve, tangent to it. Additionally, a circular arc is added at the beginning of the B-Spline curve , also tangent to the B-Spline curve. The circular arc radius, the B-Spline control points' coordinates and the length of the B-Spline extension, are defined in a non-dimensional form, using as reference lengths the horizontal and vertical distances between the first and last control points of the B-Spline curve. These lengths will be correspondingly called reference axial length L and offset O during the rest of the paper.

The offset (Oef) is fixed during the design procedure, as it is determined by the diameter of the UAV fuselage and the position of the jet engine . The maximum allowable value of the reference axial length (Lax,ref) is also predetermined and provided as a design constraint . The minimum allowable value of the reference axial length (Lax,ref) is defined by the requirement the S-bent of the duct to fit into the flow diverter, positioned between the cowl and the UAV fuselage. Additionally, a very sharp bend will considerably increase the total pressure losses

and the flow distortion at the engine face, as it will be demonstrated in the following sections.

Nomenclature

A = duct cross-sectional area

C = sonic velocity

CP = static pressure coefficient

CPO = total pressure coefficient

d = inlet duct diameter

H = boundary layer shape factor (***S1&/S2)***

M = Mach number

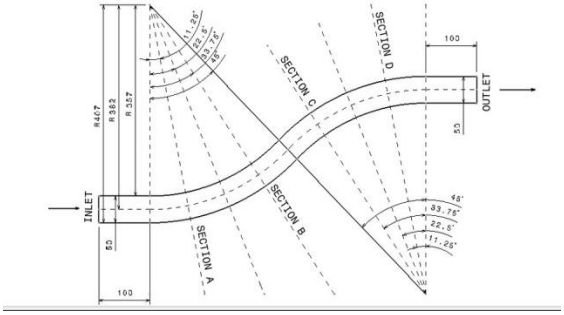

Fig: Nomenclature of S- Duct

- **Mach number**
  - **M =** $\frac{V/c}{m}$
- **Total pressure coefficient**
  - **Cpo =** $\frac{Po-Pcl}{Po,cl-Pcl}$
- **Static pressure coefficient**
  - **Cp =** $\frac{P-Pel}{Po,cl-Pcl}$

Along the B-Spline curve several duct profiles are constructed, at planes normal to the curve. Their position is non-dimensionally defined as a fraction of curve's length. In four such profiles are plotted, with the first and last corresponding to the 0 and 100 percent of B-Spline's length, respectively. The first profile is transported along the circular arc, in order to form the profile at the duct entrance. A last (circular) profile is defined at the end of the straight line extension of the B-Spline curve, which corresponds to the jet engine's face. Various profile types can be used, such as rounded orthogonal, rounded trapezoidal, circular, elliptical, or special profiles defined by B-Spline curves. All the profiles are defined using geometric parameters, non-dimensionalized with the duct radius at the engine face. In this way, the scaling of the duct, in order to fit to a different engine's face, becomes a fully automated procedure. The internal surface of the S-duct is constructed, using as reference curves the aforementioned profiles.

The throat Mach number Mt,d is needed in order to determine the throat area At of the intake. The latter corresponds to the profile at the start of the centre line. For the determination of At we use one-dimensional calculations, from the far upstream to the throat. As the static flow quantities far upstream are known for the specified flight Mach number and altitude (assuming Standard Atmosphere), the corresponding total flow quantities can be computed, using free stream Mach number. The throat total temperature is defined by assuming adiabatic flow between the far upstream position and the throat. The throat total pressure is defined by assuming a pre-specified total pressure loss between the far upstream and the throat, equal to 0.2 percent. Using isentropic relations and the predefined throat Mach number, the static flow quantities pt, Tt, rt can be computed along with the speed of soundat the throat, and the mean flow velocity. Subsequently, using the engine mass flow rate and the continuity equation, the throat area At can be easily derived. The capture area Ac at the lip face can be specified if a contraction ratio CR ¼ At/Ac is assumed between the lip and the throat. A value of CR around 0.75 was selected, in order to obtain a compromise design for both high and low flight speeds. By assuming such a value for the contraction ratio, the possibility of lip separation at zero speed is minimized.

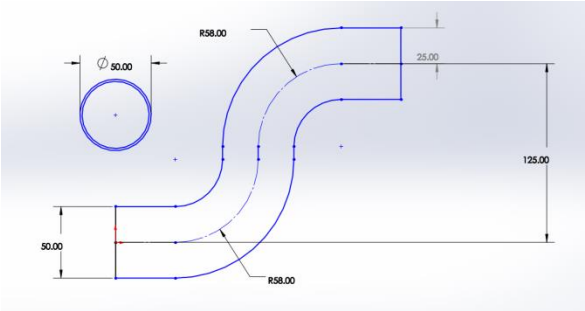

Fig: Diagram of Cross sectional view of Circular S-Duct.

The latter is an essential request in the case of a UAV; the lip separation results in a reduction of the intake efficiency, and consequently the engine thrust during the UAV's launching phase, when the maximum available thrust is needed. As it was mentioned before, the internal lip profile is an elliptical one with the major axis in the flow direction. An ellipse major to minor axis ratio a/b equal to 3.0 was used in the present design. By defining the small axis and the throat profile, the capture area is automatically computed and the resulting contraction ratio is verified. The most significant design parameters are summarized .The intake profile at the engine face is a circular one, defined by the engine face diameter Def . The previous one is also a circular one; in general its diameter is specified in such a way to produce a convergence rate at the last part of the intake almost the same to the one at the engine inlet

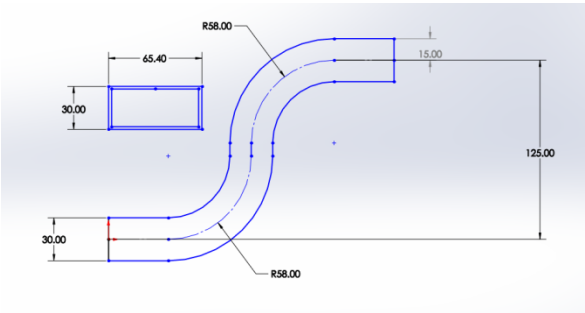

Fig: Diagram of Cross sectional view of Rectangular S- Duct

In our case this profile was set to have the same diameter with the one at the engine face. The intake convergence and the corresponding flow acceleration are needed in order to minimize the flow distortion at the engine face; the straight line extension of the B-Spline curve is adopted for the same reason. A rectangular cross-section with rounded corners was adopted for the throat section. This selection was the result of the requirement to keep the vertical height of the cowl as low as possible. An additional reason for the selection of a rectangular cross-section was the horizontal separation of the secondary vortices that this configuration can provide , which leads to a more uniform flow field at the face of the compressor. Imposing an elliptic profile for the internal surface of the lip of the intake , a similar rounded rectangular cross-section resulted for the capture plane.

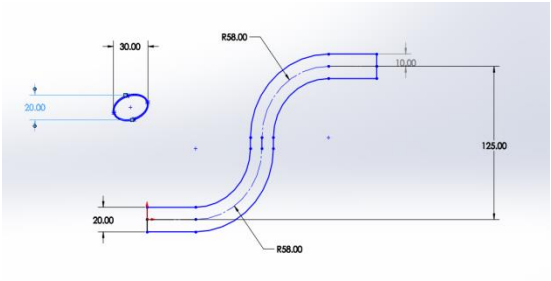

Fig: Diagram of Cross sectional view of Ellipse S- Duct

In order to materialize a Gerlach area shaping for the duct and provide a smooth and controllable area variation between the throat and engine face, two additional cross-sectional profiles were defined in planes normal to the B-Spline part of the centre line. These profiles correspond to positions 2 and 3 and are defined in planes normal to the centre line; their position is provided as a fraction of B-Spline's curve length. At the first bend of the duct, due to the pressure gradient existing between inner and outer walls , the boundary layer from the outside of the first bend moves towards the inside of the duct. As a result some swirl is generated at the engine face (Seddon and Goldsmith, 1999). Gerlach shaping consists of designing the duct cross-section so that velocity is increased at the outer wall and decreased at the inner wall of the first bend. This is realized by narrowing the duct at the outer wall and widening it at

the inner wall, with respect to its cross-section at the throat. As a result, the pressure gradient between the walls is reduced, along with the extended of separation, without changing mean flow velocity.

Methodology

The main flow domain of the S-duct (from duct inlet to the engine face) was modelled in CATIA V5, as described earlier, and imported to ANSYS ICEM CFD commercial mesh generation software. An additional cylindrical part, common to all cases considered, containing engine inlet and the corresponding engine bullet, was constructed

- The rounded of the bullet was constructed using a spherical sector, in a way to maintain curvature continuity between the sphere and the cone at their interface.
- Rectangle section axial length Lax,eng was set equal to 500 mm. The rectangle with a base diameter length L is 65.4 mm breadth B 30 mm and a height Lax,bul equal to 1.288B.
- Ellipse section axial length Lax,eng was set equal to 500 mm. The ellipse with a base diameter length A is 20.8 mm breadth B 30 mm and a height Lax,bul equal to 1.288A.
- Cylindrical section, Rectangular section and Ellipse section blocking methodology was used in order to construct the mesh, used in our simulations; the mesh consists of hexahedral elements.
- The adopted blocking strategy consists of making blocks for the primitive and general geometrical features and continuing to the most detailed and smaller parts of the geometry.
- A complicated block-structured topology was used for the grid construction, resulting in 39 different blocks. The blocking topology. The adopted topology enabled the construction of a fine mesh near the engine bullet wall at the engine inlet region.
- Appropriate associations were applied between the blocks and the corresponding geometry surfaces or curves in order to keep the surface representation and the mesh density variation as smooth as possible.
- The structured grids used in this study contained about approximately 490,000-640,000 hexahedral elements, according to the length of the discretized duct.
- The number of elements in each cross-section of the duct was kept almost constant in all cases, with the number of elements in the longitudinal direction varying with the axial length of the duct.

Cylindrical Type S- Duct

Area of cross section (Circle Type)

$Ac = \pi r^2$

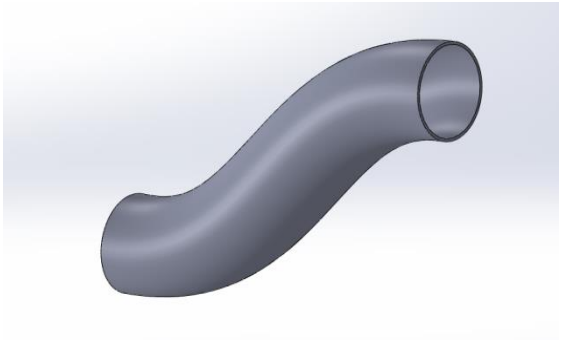

Fig: CAD Model of Circular S- Duct Design

Rectangular Type S- Duct

Area of cross section (Rectangular Type) Ar = L x B

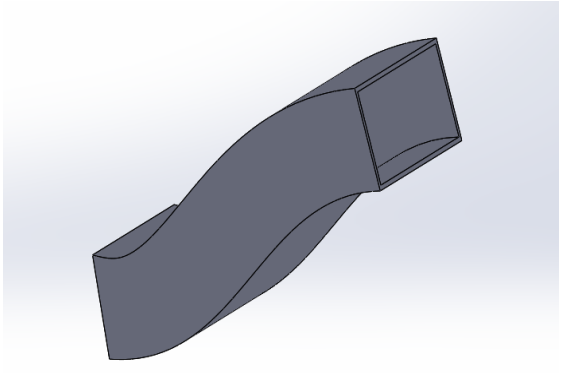

Fig: CAD Model of Rectangular S- Duct Design

Ellipse Type S- Duct

Area of cross section (Ellipse Type)

Ae = πAB

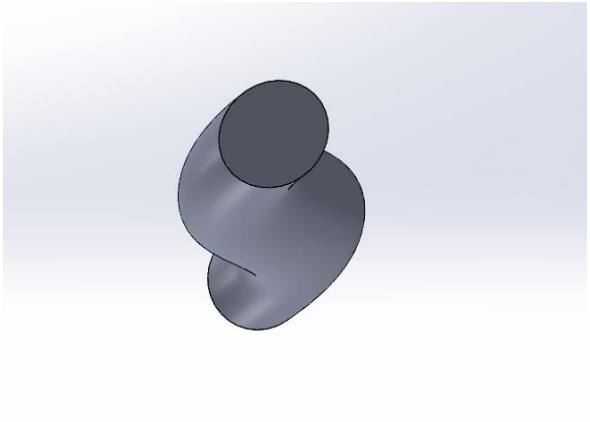

Fig: CAD Model of Ellipse S- Duct Design

CFD ANALYSIS

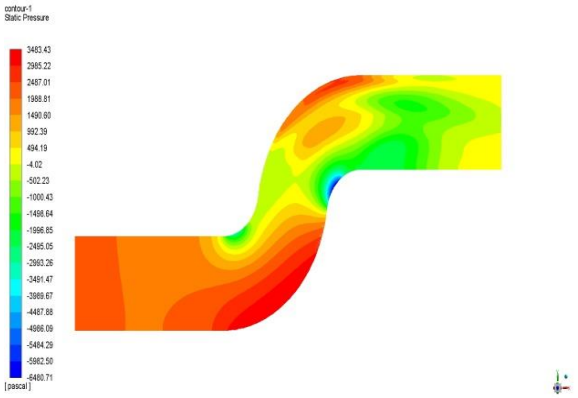

Fig: CFD analysis of Circular S-Duct Static Pressure

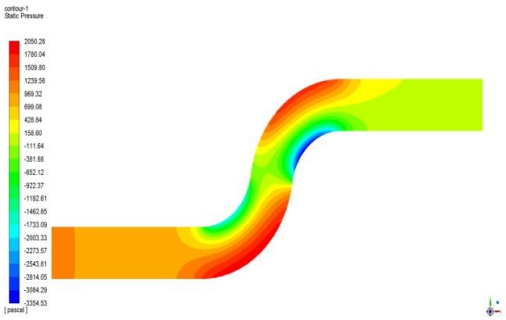

Fig: CFD analysis of Rectangular S-Duct Static Pressure

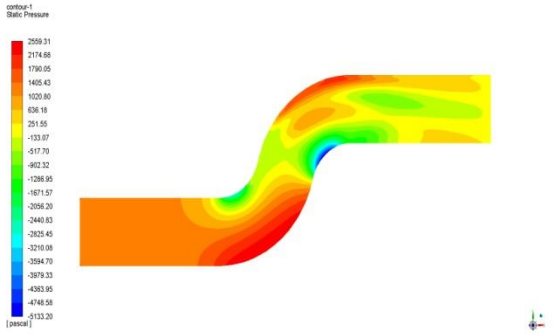

Fig: CFD analysis of Ellipse S-Duct Static Pressure

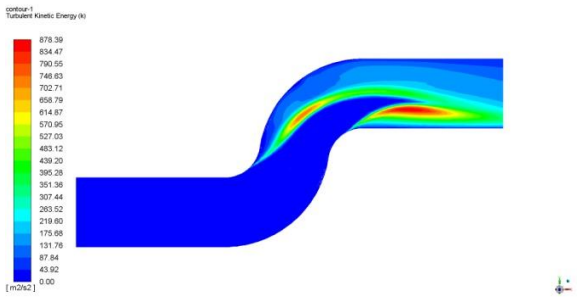

Fig: CFD analysis of Circular S-Duct Turbulent Kinetic Energy (k)

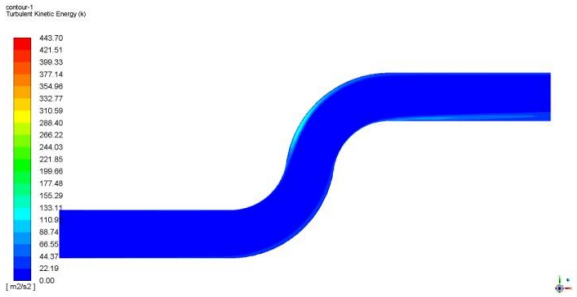

Fig: CFD analysis of Rectangular S-Duct Turbulent Kinetic Energy (k)

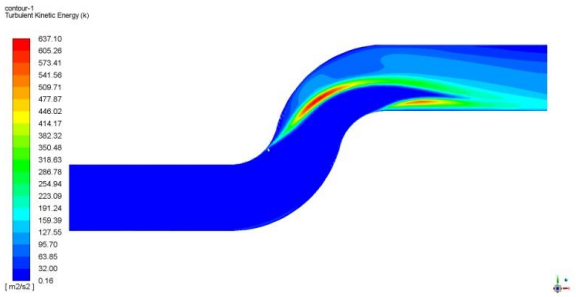

Fig: CFD analysis of Ellipse S-Duct Turbulent Kinetic Energy (k)

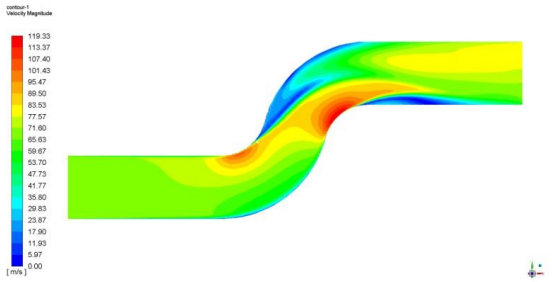

Fig: CFD analysis of Ellipse S-Duct Velocity Magnitude

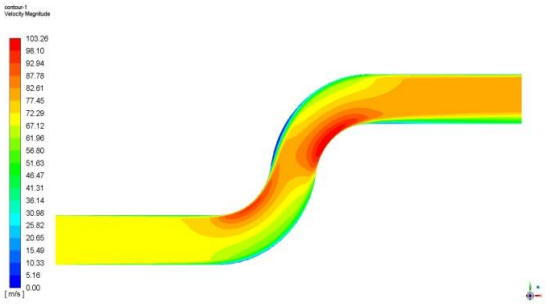

Fig: CFD analysis of Circular S-Duct Velocity Magnitude

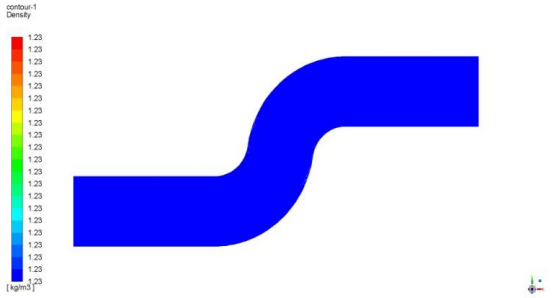

Fig: CFD analysis of Circular S-Duct Density

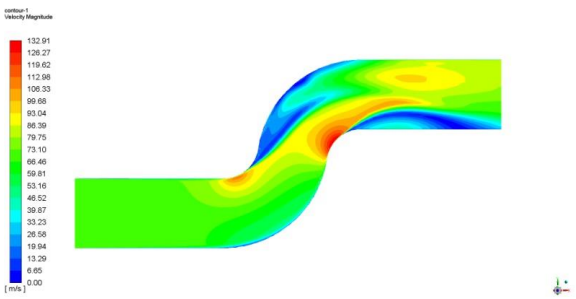

Fig: CFD analysis of Rectangular S-Duct Velocity Magnitude

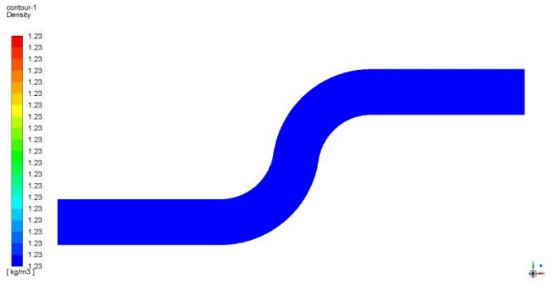

Fig: CFD analysis of Rectangular S-Duct Density

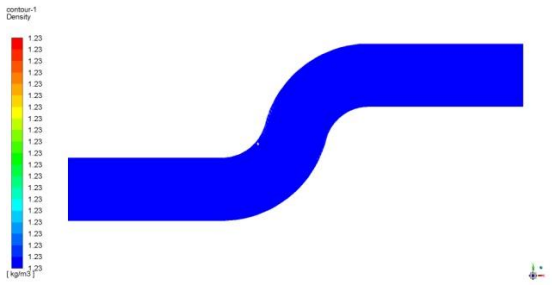

Fig: CFD analysis of Ellipse S-Duct Density

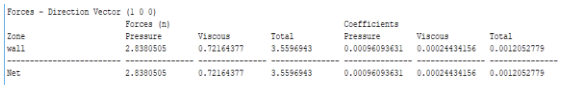

Forces - Direction Vector (1 0 0)

Zone	Forces (n) Pressure	Viscous	Total	Coefficients Pressure	Viscous	Total
wall	2.8380505	0.72164377	3.5596943	0.00096093631	0.00024434156	0.0012052779
Net	2.8380505	0.72164377	3.5596943	0.00096093631	0.00024434156	0.0012052779

Fig: CFD analysis of Circular S-Duct Drag force

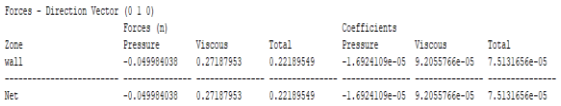

Forces - Direction Vector (0 1 0)

Zone	Forces (n) Pressure	Viscous	Total	Coefficients Pressure	Viscous	Total
wall	-0.049984038	0.27187953	0.22189549	-1.6924109e-05	9.2055766e-05	7.5131656e-05
Net	-0.049984038	0.27187953	0.22189549	-1.6924109e-05	9.2055766e-05	7.5131656e-05

Fig: CFD analysis of Circular S-Duct Lift force

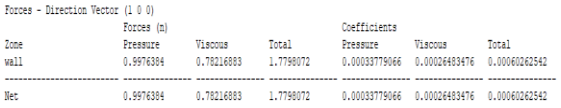

Forces - Direction Vector (1 0 0)

Zone	Forces (n) Pressure	Viscous	Total	Coefficients Pressure	Viscous	Total
wall	0.9976384	0.78216883	1.7798072	0.00033779066	0.00026483476	0.00060262542
Net	0.9976384	0.78216883	1.7798072	0.00033779066	0.00026483476	0.00060262542

Fig: CFD analysis of Rectangular S-Duct Drag force

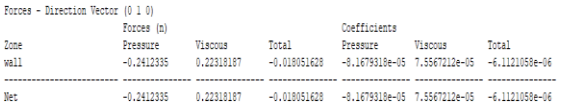

Forces - Direction Vector (0 1 0)

Zone	Forces (n) Pressure	Viscous	Total	Coefficients Pressure	Viscous	Total
wall	-0.2412335	0.22318187	-0.018051628	-8.1679318e-05	7.5567212e-05	-6.1121058e-06
Net	-0.2412335	0.22318187	-0.018051628	-8.1679318e-05	7.5567212e-05	-6.1121058e-06

Fig: CFD analysis of Rectangular S-Duct Lift force

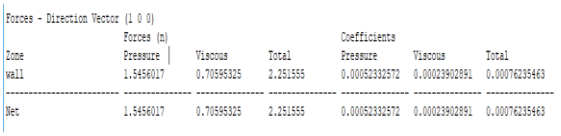

Forces - Direction Vector (1 0 0)

Zone	Forces (n) Pressure	Viscous	Total	Coefficients Pressure	Viscous	Total
wall	1.5456017	0.70595325	2.251555	0.00052332572	0.00023902891	0.00076235463
Net	1.5456017	0.70595325	2.251555	0.00052332572	0.00023902891	0.00076235463

Fig: CFD analysis of Ellipse S-Duct Drag force

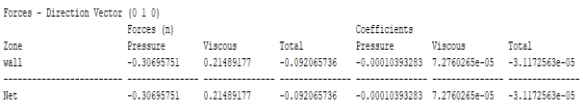

Forces - Direction Vector (0 1 0)

Zone	Forces (n) Pressure	Viscous	Total	Coefficients Pressure	Viscous	Total
wall	-0.30695751	0.21489177	-0.092065736	-0.00010393283	7.2760265e-05	-3.1172563e-05
Net	-0.30695751	0.21489177	-0.092065736	-0.00010393283	7.2760265e-05	-3.1172563e-05

Fig: CFD analysis of Ellipse S-Duct Lift force

ACKNOWLEDGEMENT

The authors wish to acknowledge the department of mechanical engineering, ponjesly college of engineering for supporting the present work. We also thank Dr. Robin Kumar Samuel., M.E, Ph.D., for their valuable suggestions.

CONCLUSIONS

- A parametric CAD model of an S-duct was initially constructed in order to identify the optimal parameters for a duct design for Aircraft and Automobile application.
- The three different shaped design was adopted in order to decrease the strength of the secondary vortices, which proved to be a good choice.
- Current study Circular section, Rectangular section and Ellipse section S- Duct CAD modelling is drawn as per test required parameters.
- The cross sectional areas are same in all shape of S- Duct.
- The CFD analysis conducted on all designs (Static Pressure, Kinetic Energy, Velocity, Density, Drag and Lift)
- After the CFD analysis complete the results shows the Ellipse section S-Duct is give better results than Circular and Rectangular section S-Duct.
- Because of the shape of ellipse is make better results output, that's make good down (drag) force. This down force will prevent cars lifts from road to air.
- Finally the Ellipse section S- Duct is best for Automobile and other transport applications.

Reference

1. Anand, R.B., Rai, L. and Singh, S.N. (2003), "Effect of the turning angle on the flow and performance characteristics of long S-shaped circular diffusers", Proceedings of the Institute of Mechanical Engineering, Part G, Journal of Aerospace Engineering, Vol. 217, pp. 29-41.

2. Baals, D.D., Smith, N.F. and Wright, J.B. (1949), The Development and Application of High-critical-speed Nose Inlets, NACA Report No. 920.
3. Bansod, P. and Bradshaw, P. (1972), "The flow in S-shaped ducts", Aeronautical Quarterly, Vol. 23, pp. 131-40.
4. Berrier, B.L. and Allan, B.G. (2004), "Experimental and computational evaluation of flush-mounted, S-duct inlets",
5. 42nd AIAA Aerospace Sciences Meeting & Exhibit Proceedings of the International Conference in Reno, NV, 5-8 January (AIAA 2004-0764).
6. Fluid Dynamics Panel Working Group 13 (1991), Air Intakes for High Speed Vehicles, AGARD-AR-270.
7. Fox, R.W. and Kline, S.J. (1962), "Flow regimes in curved subsonic diffusers", Transactions of the ASME, Journal of Basic Engineering, Vol. 84, pp. 21-8.
8. Freitas, C.J. (1995), "Perspective: selected benchmarks from commercial CFD codes", Transactions of the ASME, Journal of Fluids Engineering, Vol. 117, pp. 208-18.
9. Goldsmith, E.L., Surber, L.E., Welte, D. and Laruelle, G. (1991), "Chapter 2 – intake design and performance", Air
10. Intakes for High Speed Vehicles, AGARD, AR-270.
11. Grotjans, H. and Menter, F.R. (1998), "Wall function for general application CFD codes", in Papailiou, K.D.,
12. Tsahalis, D., Pe´riaux, J. and Kno¨ rzer, D. (Eds), ECCOMAS 98 Proceedings of the 4th Computational Fluid Dynamics Conference, Vol. 1, Willey, New York, NY, Pt. 2, pp. 1112-17.
13. Guo, R.W. and Seddon, J. (1983), "An investigation of the swirl in an S-duct", Aeronautical Quarterly, Vol. 32, pp. 99-129.
14. Iaccarino, G. (2001), "Predictions of a turbulent separated flow using commercial CFD codes", Transactions of the ASME, Journal of Fluids Engineering, Vol. 123, pp. 819-28.
15. Laruelle, G. and Goldsmith, E.L. (1993), "Chapter 8 – intakes for missiles with air-breathing propulsion", in Goldsmith,
16. E.L. and Seddon, J. (Eds), Practical Intake Aerodynamic Design, AIAA Education
17.